ACS APPLIED MATERIALS & INTERFACES

Research Article

www.acsami.org

Highly Sensitive Detection of Caspase-3 Activities via a Nonconjugated Gold Nanoparticle–Quantum Dot Pair Mediated by an Inner-Filter Effect

Jingwen Li, Xinming Li,* Xiujuan Shi, Xuewen He, Wei Wei, Nan Ma,* and Hong Chen

College of Chemistry, Chemical Engineering and Materials Science, Soochow University, Suzhou 215123, China

Supporting Information

ABSTRACT: We describe here a simple fluorometric assay for the highly sensitive detection of caspase-3 activities on the basis of the inner-filter effect of gold nanoparticles (AuNPs) on CdTe quantum dots (QDs). The method takes advantage of the high molar absorptivity of the plasmon band of gold nanoparticles as well as the large absorption band shift from 520 to 680 nm upon nanoparticle aggregation. When labeled with a peptide possessing the caspase-3 cleavage sequence (DEVD), the monodispersed Au-Ps (peptide-modified AuNPs) exhibited a tendency to aggregate when exposed to caspase-3, which induced the absorption band transition from 520 to 680 nm and turned on the fluorescence of the CdTe QDs for caspase-3 sensing. Under optimum conditions, a high sensitivity towards caspase-3 was achieved with a detection limit as low as 18 pM, which was much lower than the corresponding assays based on absorbance or other approaches. Overall, we demonstrated a facile and sensitive approach for caspase-3 detection, and we expected that this method could be potentially generalized to design more fluorescent assays for sensing other bioactive entities.

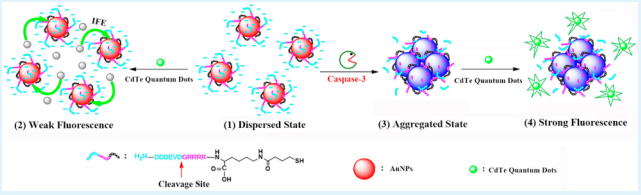

KEYWORDS: *caspase-3, inner-filter effect, gold nanoparticle, quantum dot, fluorescence*

1. INTRODUCTION

Caspases, as a family of intracellular cysteine proteases, play a critical role in regulating programmed cell death, or apoptosis.[1,2] Among them, caspase-3 has been identified as a key effector of cell apoptosis and an important indicator of the cell's entry point into the apoptotic pathway.[3−5] Since the discovery that the deregulation of cell apoptosis can ultimately lead to cancers,[6] neurodegenerative disorders,[7] chronic heart failure,[8] and many other diseases,[9,10] numerous studies have been carried out to search for effective methods of caspase-3 detection, such as through fluorometry,[11−15] colorimetry,[16,17] electrochemistry,[18] atomic force microscopy,[19] magnetic resonance imaging,[20] and nuclear imaging.[21,22] However, most of these methods suffer from laborious synthetic procedures, low sensitivity, or complicated detection facilities, which severely restricted their extensive applications for sensitive and rapid caspase-3 detection. Thus, it is highly desirable to develop efficient methods for caspase-3 detection, drug screening, or deregulated apoptosis investigation.

In this study, we report a novel fluorometric assay for the detection of caspase-3 activities on the basis of the inner-filter effect (IFE) of gold nanoparticles (AuNPs) on quantum dots (QDs). Compared to the conventional fluorescence resonance energy transfer (FRET)-based fluorometric assays for protease detection, our method does not require chemical linkage between an absorber and a fluorophore, which offers considerable flexibility and simplicity in probe fabrication and experimental design. The IFE of fluorescence refers to the absorption of the excitation and/or emission of light by absorbers in the detection system.[23] A general and feasible strategy to achieve detection sensitivity in the IFE-based fluorescent assay is to increase the spectral overlap between the fluorophore's emission and the absorber's absorption and/or to select an absorber with a high extinction coefficient. Therefore, the IFE of fluorescence has emerged as an efficient strategy for the design and development of novel probes for variable analyte detection by choosing suitable absorber−fluorophore pairs. However, so far, IFE-based detection has been mostly applied to small chemical analytes,[24−29] and the use of this strategy for the detection of more complex analytes, such as proteases, remains little explored.

Herein, we developed a simple and sensitive caspase-3 sensing system based on the IFE of AuNPs on the fluorescence of CdTe QDs, where AuNPs and CdTe QDs were chosen as the absorber−fluorophore pair to modulate the emission of the fluorophore because of the tremendously larger extinction coefficient of AuNPs as well as the brighter fluorescence and better photostability of QDs.

The principle of our experimental design and fluorescent assays are illustrated in Scheme 1 and are explained as follows. (1) A dodeca-peptide derivative (NH_2-Asp-Asp-Asp-Glu-Val-Asp-Gly-Arg-Arg-Arg-Arg-Mpa, DDDEVDGRRRR-Mpa, or

Received: July 23, 2013
Accepted: September 9, 2013
Published: September 9, 2013

   dx.doi.org/10.1021/am4029735 | ACS Appl. Mater. Interfaces 2013, 5, 9798−9802

Scheme 1. Illustration of the Fluorescent Detection of Caspase-3 through the Inner-Filter Effect of Gold Nanoparticles on Quantum Dots

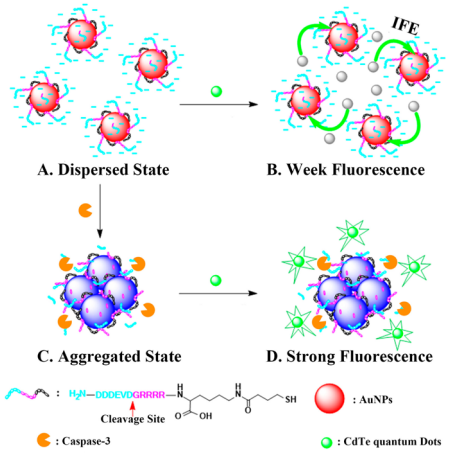

DK (Mpa)-12) consisting of a caspase-3 recognition motif (DEVD) and mercaptopropionic acid was designed to allow its efficient interaction with caspase-3 and its anchorage on the surface of AuNPs through a Au−S bond. Because of the negative charge of DK (Mpa)-12 in total at pH 7.4, the introduction of DK (Mpa)-12 to the surface of citrate-stabilized AuNPs afforded a monodispersed AuNPs solution in water (Scheme 1A). (2) Because of the large overlap of the absorption of peptide-modified AuNPs (Au-Ps) with the emission of CdTe QDs at 520 nm, the fluorescence of CdTe QDs was quenched properly in the mixture solution of Au-Ps and CdTe QDs without the presence of caspase-3 (Scheme 1B). (3) Upon the addition of caspase-3, a negatively charged peptide segment (NH_2-Asp-Asp-Asp-Glu-Val-Asp-OH) was enzymatically removed from the Au-Ps surface (Scheme 1), resulting in the coverage of the positive charged peptide (NH_2-Gly-Arg-Arg-Arg-Arg-Mpa) on the surface of Au-Ps for Au nanoparticle aggregation via electrostatic interactions (Scheme 1C). As a result, the fluorescence emission of CdTe QDs was restored properly for caspase-3 detection (Scheme 1D), and its intensity displayed a good linear relationship with caspase-3 concentration. Because the absorbance transition of Au-Ps led to the increase of the fluorescence intensity of QDs exponentially, an enhanced sensitivity for the detection of caspase-3 was achieved with a detection limit around 18 pM, which is much lower than the previously reported colorimetric assay based on unmodified gold nanoparticles.[17]

2. MATERIALS AND METHODS

Sodium citrate tribasic dehydrate ($Na_3Ct{\cdot}2H_2O$, 99.0%), cadmium chloride ($CdCl_2$, 99.99%), tellurium powder (Te, 99.997%), sodium borohydride ($NaBH_4$, 98%), and glutathione (GSH, 95%) were purchased from Sigma. Human recombinant caspase-3 was purchased from R&D Systems (Minneapolis, MN). The peptide sequence (NH_2-Asp-Asp-Asp-Glu-Val-Asp-Gly-Arg-Arg-Arg-Arg-Mpa (DDDEVDGRRRR-Mpa, DK (Mpa)-12)), which served as the substrate for caspase-3, was provided by GL Biochem, Ltd. (Shanghai, China). Other reagents were obtained from Sinopharm Chemical Reagent Company of China and were used as received. All solutions were prepared with ultrapure water (18.2 MΩ cm) from a Millipore system. Centrifugation was carried out on an eppendorf 5810R centrifuge. The absorption spectra were obtained on an Agilent 8453 UV−vis spectrophotometer and Thermo Scientific Varioskan Flash spectral scanning multimode reader. Fluorescence emission spectra were recorded on a fiber fluorescence spectrophotometer (AvaSpec-ULS2048-USB2) equipped with a UV excitation light source (excitation 405 nm). Transmission electron microscopy (TEM) characterization was performed using a JEOL JEM-2100 transmission electron microscope operating at 200 kV. Zeta potentials were measured on a Malvern Zetasizer Nano ZS90.

Synthesis of CdTe QDs. Fresh sodium hydrogen telluride (NaHTe) solution was made before each synthesis by dissolving 0.025 g of sodium borohydride ($NaBH_4$) in 1 mL of deionized water followed by the addition of 0.040 g of tellurium powder, and the solution was heated at 60 °C for 40 min. The $CdCl_2$-GSH stock solution (1.25 mM $CdCl_2$ and 1.05 mM GSH) was prepared by dissolving 1.2 mg of $CdCl_2$ and 1.6 mg of GSH in 5 mL of H_2O, and the pH was adjusted to 9.0 with sodium hydroxide before use. Next, 400 μL of the $CdCl_2$-GSH stock solution was mixed with 0.8 μL of a freshly prepared NaHTe solution in a glovebox (Etelax, Lab2000). The reaction mixture was then heated at 100 °C and reacted for 30 min before cooling to room temperature. The resulting GSH-capped CdTe QDs were characterized by TEM, UV−vis spectroscopy, fluorescence emission spectrum (Figure S1), and zeta potential analysis. The concentration of CdTe QDs was estimated to be 1.41×10^{-6} M according to a previous report.[30]

Synthesis of Gold Nanoparticles (AuNPs). Citrate-stabilized AuNPs were prepared by following Frens' method, as reported previously.[31] All glassware used in the experiment was soaked in aqua regia, rinsed thoroughly with water, and oven-dried prior to use. In brief, a 50 mL aqueous solution of $HAuCl_4$ (0.25 mM) was heated to boiling followed by the addition of 1.6 mL of trisodium citrate (1%) with vigorous stirring. The solution was maintained at the boiling state for 10 min, during which time the color changed from yellow to deep wine red. A stable and monodispersed gold nanoparticle colloidal solution was obtained and stored at 4°C. The resulting AuNPs were characterized by TEM and UV−vis spectroscopy (Figure S2). The final concentration of AuNPs was estimated to be 1.12×10^{-9} M from the UV−vis absorption spectrum based on an extinction coefficient of 7.76×10^8 M^{-1} cm^{-1} at λ_{520} for 18 nm AuNPs.[32]

Modification of AuNPs with Peptides. A 2 mM stock solution of DK (Mpa)-12 was prepared by dissolving 10.2 mg of DK (Mpa)-12 in 3.155 mL of phosphate buffer (pH 7.4, 160 mM NaCl, 3 mM KCl, 8 mM Na_2HPO_4, and 1 mM KH_2PO_4). The resulting solution was kept in a freezer (−20 °C). Peptide-functionalized gold nanoparticles (Au-Ps) were prepared by mixing the citrate gold nanoparticles and peptide stock solution in a mole ratio of 1 to 150, and the mixture was stirred at room temperature for 10 h. For the removal of excess peptides, peptide-coated particles were subjected to centrifugation at 10 000 rpm for 10 minutes, and the procedure was repeated three times. The Au-Ps pellet was redissolved in the initial volume of 0.1× phosphate buffer for experimental use and further studies. The obtained particles were characterized by TEM, UV−vis spectroscopy, and zeta potential analysis. The Au-Ps solution was mixed with CdTe QDs in different mole ratios. The emission spectra and absorption spectra were recorded.

Enzymatic Assays of Caspase-3 with Au-Ps and CdTe QDs. Caspase-3 in different concentrations was prepared by diluting the commercial stock solution of caspase-3 with 0.1× TBS (pH 7.4, 2.5 mM Tris, and 15 mM NaCl) at 202.95, 166.05, 129.15, 110.7, 92.25, 73.8, 55.35, 36.9, 27.68, and 12.3 pM, respectively. One hundred microliters of a Au-Ps solution was mixed with 20 μL of caspase-3 at different concentrations and incubated for 1 h at 37 °C. The color change of the solution was recorded with a camera, and the absorption spectroscopy measurements were performed. The sample without the presence of caspase-3 was used as a control.

One hundred microliters of a Au-Ps solution after enzymatic reaction was mixed with CdTe QDs (1.14×10^{-8} M) in a mole ratio of 1.0 to 1.0. The emission spectra were then recorded with the excitation at 405 nm. The fluorescence data were analyzed by plotting the relative fluorescence intensity (F/F_0) at 520 nm versus the concentration of caspase-3.

dx.doi.org/10.1021/am4029735 | ACS Appl. Mater. Interfaces 2013, 5, 9798−9802

3. RESULTS AND DISCUSSION

From the absorption spectrum of Au-Ps shown in Figure 1, we found that the aqueous pink solution of Au-Ps displayed

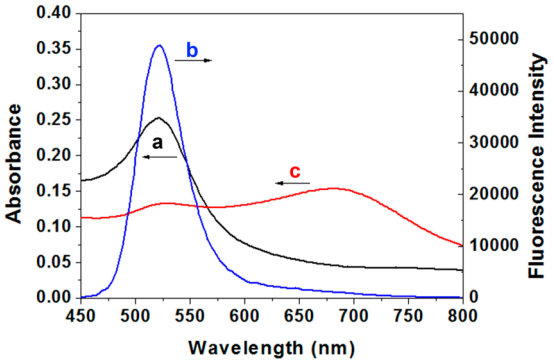

Figure 1. (a) Absorption spectrum of Au-Ps, (b) fluorescence emission spectrum of GSH-capped CdTe QDs, and (c) absorption spectrum of Au-Ps in the presence of caspase-3.

intense characteristic surface plasmon absorption at 520 nm. The average diameter of the Au-Ps obtained was about 18 nm according to the TEM image (Figure 4B). The water-soluble GSH-capped CdTe QDs were prepared through aqueous-phase synthesis,[33] and they showed a fluorescence emission maximum at 520 nm, which overlapped very well with the absorption spectrum of Au-Ps to induce IFE between them. However, upon the addition of caspase-3, Au-Ps tended to aggregate together because of the enzymatic cleavage reaction of the DEVD-motif-containing peptide and resulted in the shift of the absorption band of the Au-Ps from 520 to 680 nm (Figure 1), restoring the fluorescence emission of CdTe QDs for caspase-3 detection.

To analyze the conjugation mode between DK (Mpa)-12 and AuNPs, we used FTIR spectroscopy to characterize the citrate-stabilized AuNPs and Au-Ps. From the spectra shown in Figure 2A, we found that the two spectra showed similar characteristics for most of the peaks except for two additional bands around 1650 and 3266 cm^{-1} on the spectrum of Au-Ps, which belonged to the stretching vibrations of −NHCO− and −NH− groups, respectively, from the DK (Mpa)-12 peptide. In addition, the disappearance of −SH vibration around 2550−2670 cm^{-1} on the Au-Ps also signified the successful attachment of DK (Mpa)-12 onto the AuNPs.[34] The results of agarose gel electrophoresis (Figure 2B) further confirmed the successful conjugation of peptides with AuNPs for the generation of Au-Ps. After modification with the peptide DK (Mpa)-12, the Au-Ps exhibited a faster electrophoretic mobility than that of the naked AuNPs because of the increase in the surface negative charges.

To verify the existence of the IFE between Au-Ps and CdTe QDs, we incubated CdTe QDs with different concentrations of Au-Ps and monitored the fluorescence changes of the CdTe QDs. As shown in Figure 3, we observed a gradual decrease of the fluorescence emission intensity from CdTe QDs with the increment of the concentration of Au-Ps. For example, when the concentration of Au-Ps was increased to 1.12×10^{-9} M, more than 60% of the fluorescence emission from CdTe QDs (1.14 × 10− M) was quenched properly. Because the absorption spectrum of Au-Ps overlaps well with the fluorescence emission spectrum of CdTe QDs, the fluorescence emission of CdTe QDs will be substantially decreased by Au-Ps

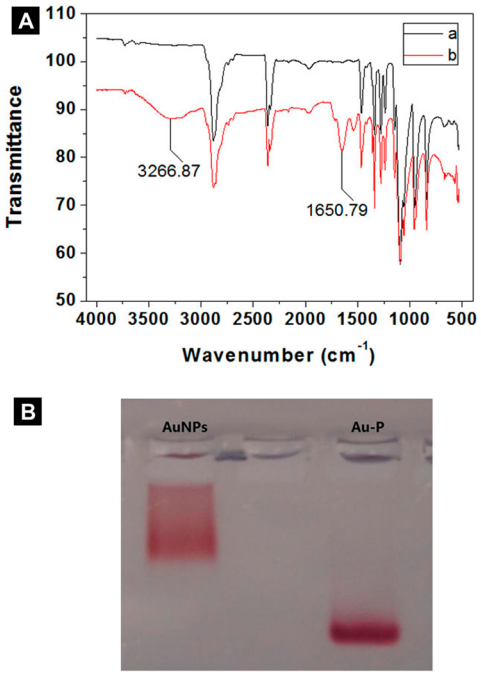

Figure 2. (A) FTIR spectra of citrate-stabilized AuNPs (a) and peptide-modified AuNPs (Au-Ps) (b). (B) Agarose gel electrophoresis of citrate-stabilized AuNPs and Au-Ps.

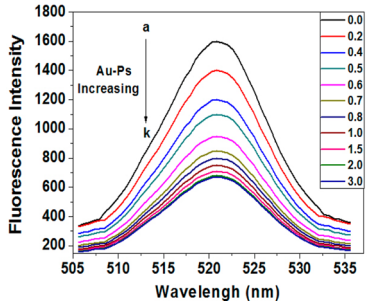

Figure 3. Fluorescence emission spectra of GSH-capped CdTe QDs incubated with Au-Ps of different concentrations. The concentrations of Au-Ps in the samples (a−k) are K × 10^{-9} M (K = 0, 0.22, 0.45, 0.56, 0.67, 0.78, 0.90, 1.12, 1.68, 2.24, and 3.36, respectively), and the corresponding mole ratios of Au-Ps to CdTe QDs in the samples (a−k) are 0.0, 0.2, 0.4, 0.5, 0.6, 0.7, 0.8, 1.0, 1.5, 2.0, and 3.0. (CdTe QDs, 1.14×10^{-8} M, λ_{ex} = 405 nm).

when they exist together. In addition, because both Au-Ps and CdTe QDs showed negative zeta potentials at pH 7.4 (Figure S3) and the absorption spectra of Au-Ps remained unchanged in the presence of CdTe QDs (Figure S4), there is no electrostatic attractive interaction for complex formation or rare energy transfer between the CdTe QDs and Au-Ps.[35] Therefore, we confirmed that the observed fluorescence decrease was not a result of the FRET process between the CdTe QDs and Au-Ps but was because of the IFE of Au-Ps on the fluorescence of CdTe QDs.

The absorption spectra changes of Au-Ps induced by caspase-3 were studied with UV spectroscopy and are shown in Figure 4A. In the presence of caspase-3, the peptide (DK (Mpa)-12) capped on AuNPs was susceptible to enzymatic cleavage on the DEVD motif, resulting in Au-Ps aggregation. From the absorption spectrum, we can find a gradual transition of the absorption band of Au-Ps from 520 to 680 nm and a decreased

dx.doi.org/10.1021/am4029735 | ACS Appl. Mater. Interfaces 2013, 5, 9798−9802

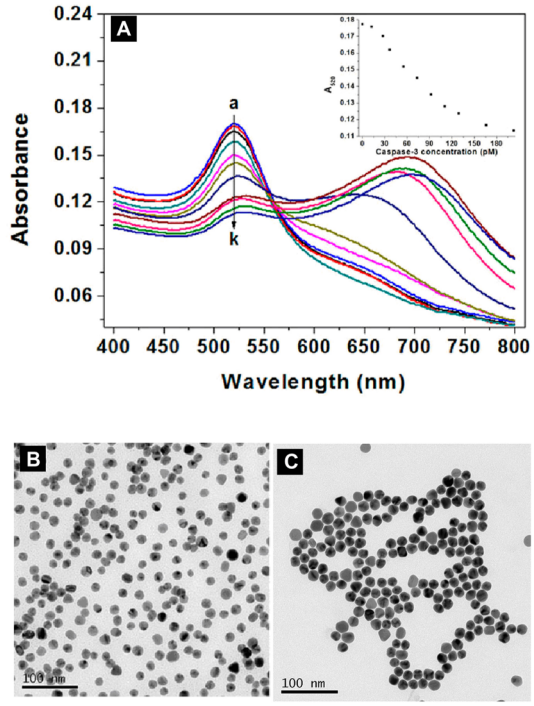

Figure 4. (A) Absorption spectrum of Au-Ps (1.12×10^{-9} M) upon the addition of caspase-3 at different concentrations (a–k) at K × 10^{-12} M (K = 0, 12.3, 27.68, 36.9, 55.35, 73.8, 92.25, 110.7, 129.15, 166.05, and 202.95). The inset shows the absorbance intensity of Au-Ps at 520 nm versus the concentration of caspase-3. (B, C) TEM images of Au-Ps before (B) and after (C) addition of caspase-3.

absorbance intensity of Au-Ps at 520 nm (inset curve in Figure 4A) with the increase of caspase-3 concentration as a result of the Au-Ps aggregation process. Such a process was also confirmed by the obvious color change of the Au-Ps solution from red to purple from visual observation (Figure S5). In addition, with the aid of transmission electron microscopy (TEM), we easily observed the aggregation of Au-Ps induced by caspase-3. Upon the addition of caspase-3, the monodispersed Au-Ps tend to aggregate together to form an Au nanoparticle complex (Figure 4B,C), which was consistent with the spectra changes shown in Figure 4A.

Although the aggregation and corresponding color change of AuNPs driven by caspase-3 have been employed for the visual sensing of caspase-3,[17] this colorimetric technique generally displays a lower sensitivity than that of fluorescence analytical methods for the detection of caspase-3 or other biomolecules.[11,13,15,36] By means of the inner-filter effect of AuNPs on QDs, an enhanced sensitivity for the detection of caspase-3 was achieved. As shown in Figure 5A, the fluorescence emission from CdTe QDs increased gradually with the increment of caspase-3 concentration, which corresponded with the decrease of the plasmon absorbance of Au-Ps at 520 nm. In addition, a good linear relationship between the relative fluorescence intensity (F/F_0) and the caspase-3 concentration was obtained in the range between 27.68 and 129.15 pM (Figure 5B), which is close to its physiologically relevant concentrations.[37,38] Furthermore, the detection limit could reach 18 pM, which was much lower than the previously reported assay for caspase-3 detection (Figure 5C).[11,15,17] Besides, the Abs 650/Abs 520 calculated from the absorption spectra of AuNPs and F/F_0 of

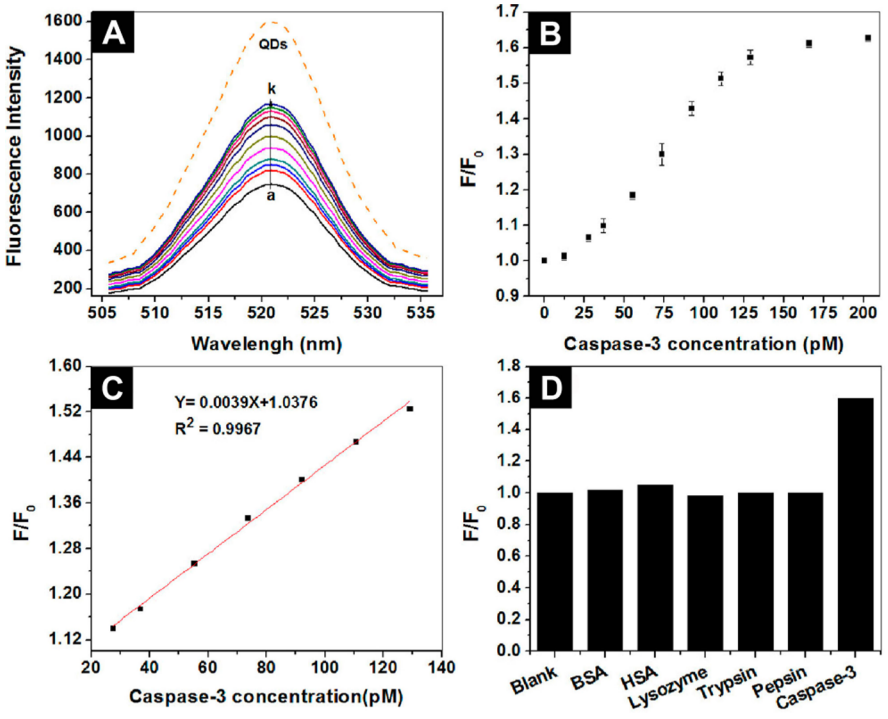

Figure 5. (A) Fluorescence emission spectra of Au-Ps–QDs system upon the addition of caspase-3 at different concentrations (a–k) at K × 10^{-12} M (K = 0, 12.3, 27.68, 36.9, 55.35, 73.8, 92.25, 110.7, 129.15, 166.05, and 202.95, respectively). (B) Plot of the relative fluorescence intensity (F/F_0) at 520 nm versus the concentration of caspase-3. (C) Linear plot of the relative fluorescence intensity (F/F_0) at 520 nm of the Au-Ps–QDs system versus the concentration of caspase-3 ranging from 27.68 to 129.15 pM. (D) Relative fluorescence intensity (F/F_0) at 520 nm of Au-Ps–QDs in the presence of various enzymes at 129.15 pM (CdTe QDs, 1.14×10^{-8} M; λ_{ex} = 405 nm; Au-Ps, 1.12×10^{-9} M).

dx.doi.org/10.1021/am4029735 | ACS Appl. Mater. Interfaces 2013, 5, 9798–9802

Au-Ps−QDs as a function of enzymatic reaction time was shown in Figure S6.

To explore the specificity of the proposed approach on the basis of the IFE of AuNPs on the fluorescence of CdTe QDs, we treated our system with other nonspecific proteins and enzymes, such as bovine serum albumin (BSA), human serum albumin (HSA), lysozyme, trypsin, and pepsin, under the same conditions. The relative fluorescence intensity (F/F_0) of CdTe QDs in the presence of different kinds of proteins and enzymes is shown in Figure 5D. It can be seen that only caspase-3 generated an increased fluorescence signal, whereas there is nearly no detectable fluorescence change upon the addition of other enzymes at the identical concentration. Thus, the Au-Ps−CdTe QDs system exhibited a good selective fluorescence response toward caspase-3.

4. CONCLUSIONS

In this work, we have demonstrated the development of a simple and sensitive caspase-3 detection system relying on the inner-filter effect of AuNPs on CdTe QDs for the first time. Upon the addition of caspase-3, which induced the aggregation of AuNPs and decreased their characteristic surface plasmon absorption at 520 nm, the fluorescence emission of CdTe QDs was restored significantly. Under optimum conditions, a high sensitivity towards caspase-3 was achieved with a detection limit as low as 18 pM, which was much lower than the previously reported assay.[11,15,17] Because of the extremely high extinction coefficient of AuNPs, the strong fluorescence of QDs, and the considerable flexibility and simplicity in the experimental design, this study illustrates a facile and sensitive approach for caspase-3 detection, and the strategy involved can be potentially generalized to design more fluorescent assays for sensing other bioactive entities.

■ ASSOCIATED CONTENT

Supporting Information

TEM images, zeta potential analyses, UV absorption spectra, and fluorescence emission spectra of peptide-modified AuNPs and CdTe QDs. This material is available free of charge via the Internet at http://pubs.acs.org.

■ AUTHOR INFORMATION

Corresponding Authors

*Tel: 86-0512-6588-2917. E-mail: xinmingli@suda.edu.cn (X.L.).

*E-mail: nan.ma@suda.edu.cn (N.M.).

Notes

The authors declare no competing financial interest.

■ ACKNOWLEDGMENTS

We thank the support of this work by the National Science Fund for Distinguished Young Scholars (201125418), the National Science Foundation of China (21175147), the Project of Scientific and Technologic Infrastructure of Suzhou (SZS201207), and the Priority Academic Program Development of Jiangsu Higher Education Institutions (PAPD).

■ REFERENCES

(1) Grütter, M. G. *Curr. Opin. Struct. Biol.* **2000**, *10*, 649−655.
(2) Vaux, D.; Korsmeyer, S. *Cell* **1999**, *96*, 245−254.
(3) Budihardjo, I.; Oliver, H.; Lutter, M.; Luo, X.; Wang, X. D. *Annu. Rev. Cell Dev. Biol.* **1999**, *15*, 269−290.
(4) Green, D. R. *Cell* **1998**, *94*, 695−698.
(5) Thornberry, N. A.; Lazebnik, Y. *Science* **1998**, *281*, 1312−1316.
(6) Kuida, K.; Zheng, T. S.; Na, S.; Kuan, C.-Y.; Yang, D.; Karasuyama, H.; Rakic, P.; Flavell, R. A. *Nature* **1996**, *384*, 368−372.
(7) Mattson, M. P. *Nat. Rev. Mol. Cell Biol.* **2000**, *1*, 120−130.
(8) Narula, J.; Pandey, P.; Arbustini, E.; Haider, N.; Narula, N.; Kolodgie, F. D.; Dal Bello, B.; Semigran, M. J.; Bielsa-Masdeu, A.; Dec, G. W. *Proc. Natl. Acad. Sci. U.S.A.* **1999**, *96*, 8144−8149.
(9) Elmore, S. *Toxicol. Pathol.* **2007**, *35*, 495−516.
(10) Kerr, J. F.; Wyllie, A. H.; Currie, A. R. *Br. J. Cancer* **1972**, *26*, 239−257.
(11) Boeneman, K.; Mei, B. C.; Dennis, A. M.; Bao, G.; Deschamps, J. R.; Mattoussi, H.; Medintz, I. L. *J. Am. Chem. Soc.* **2009**, *131*, 3828−3829.
(12) Huang, R.; Wang, X.; Wang, D.; Liu, F.; Mei, B.; Tang, A.; Jiang, J.; Liang, G. *Anal. Chem.* **2013**, *85*, 6203−6207.
(13) Liu, J.; Bhalgat, M.; Zhang, C.; Diwu, Z.; Hoyland, B.; Klaubert, D. H. *Bioorg. Med. Chem. Lett.* **1999**, *9*, 3231−3236.
(14) Shi, H.; Kwok, R. T. K.; Liu, J.; Xing, B.; Tang, B. Z.; Liu, B. *J. Am. Chem. Soc.* **2012**, *134*, 17972−17981.
(15) Wang, H.; Zhang, Q.; Chu, X.; Chen, T.; Ge, J.; Yu, R. *Angew. Chem., Int. Ed.* **2011**, *50*, 7065−7069.
(16) Gurtu, V.; Kain, S. R.; Zhang, G. *Anal. Biochem.* **1997**, *251*, 98−102.
(17) Pan, Y.; Guo, M.; Nie, Z.; Huang, Y.; Peng, Y.; Liu, A.; Qing, M.; Yao, S. *Chem. Commun.* **2012**, *48*, 997−999.
(18) Zhang, J.-J.; Zheng, T.-T.; Cheng, F.-F.; Zhu, J.-J. *Chem. Commun.* **2011**, *47*, 1178−1180.
(19) Kihara, T.; Nakamura, C.; Suzuki, M.; Han, S.-W.; Fukazawa, K.; Ishihara, K.; Miyake, J. *Biosens. Bioelectron.* **2009**, *25*, 22−27.
(20) Mizukami, S.; Takikawa, R.; Sugihara, F.; Hori, Y.; Tochio, H.; Wälchli, M.; Shirakawa, M.; Kikuchi, K. *J. Am. Chem. Soc.* **2008**, *130*, 794−795.
(21) Belhocine, T.; Steinmetz, N.; Hustinx, R.; Bartsch, P.; Jerusalem, G.; Seidel, L.; Rigo, P.; Green, A. *Clin .Cancer Res* . **2002**, *8*, 2766−2774.
(22) Haimovitz-Friedman, A.; Yang, T.-I. J.; Thin, T. H.; Verheij, M. *Radiat. Res.* **2012**, *177*, 467−482.
(23) Yuan, P.; Walt, D. R. *Anal. Chem.* **1987**, *59*, 2391−2394.
(24) Cao, X.; Shen, F.; Zhang, M.; Guo, J.; Luo, Y.; Li, X.; Liu, H.; Sun, C.; Liu, J. *Food Control* **2013**, *34*, 221−229.
(25) Li, B. *Analyst* **2012**, *137*, 3293−3299.
(26) Shang, L.; Dong, S. *Anal. Chem.* **2009**, *81*, 1465−1470.
(27) Xu, L.; Li, B.; Jin, Y. *Talanta* **2011**, *84*, 558−564.
(28) Zhang, D.; Dong, Z.; Jiang, X.; Feng, M.; Li, W.; Gao, G. *Anal. Methods* **2013**, *5*, 1669−1675.
(29) Zhang, Q.; Qu, Y.; Liu, M.; Li, X.; Zhou, J.; Zhang, X.; Zhou, H. *Sens. Actuators, B* **2012**, *173*, 477−482.
(30) Yu, W. W.; Qu, L. H.; Guo, W. Z.; Peng, X. G. *Chem. Mat.* **2003**, *15*, 2854−2860.
(31) Ghosh, S. K.; Pal, A.; Kundu, S.; Nath, S.; Pal, T. *Chem. Phys. Lett.* **2004**, *395*, 366−372.
(32) Liu, X.; Atwater, M.; Wang, J.; Huo, Q. *Colloids Surf., B* **2007**, *58*, 3−7.
(33) Ma, N.; Sargent, E. H.; Kelley, S. O. *Nat. Nanotechnol.* **2009**, *4*, 121−125.
(34) Lin, S.-Y.; Liu, S.-W.; Lin, C.-M.; Chen, C.-H. *Anal. Chem.* **2002**, *74*, 330−335.
(35) Wang, X.; Guo, X. *Analyst* **2009**, *134*, 1348−1354.
(36) Xie, X.; Xu, W.; Liu, X. *Acc. Chem. Res.* **2012**, *45*, 1511−1520.
(37) Pop, C.; Chen, Y. R.; Smith, B.; Bose, K.; Bobay, B.; Tripathy, A.; Franzen, S.; Clark, A. C. *Biochemistry* **2001**, *40*, 14224−14235.
(38) Stennicke, H. R.; Jurgensmeier, J. M.; Shin, H.; Deveraux, Q.; Wolf, B. B.; Yang, X. H.; Zhou, Q.; Ellerby, H. M.; Ellerby, L. M.; Bredesen, D.; Green, D. R.; Reed, J. C.; Froelich, C. J.; Salvesen, G. S. *J. Biol. Chem.* **1998**, *273*, 27084−27090.